Journal of Asian Concrete Federation

journal homepage: https://jacf.sfulib3.publicknowledgeproject.org/index.php/jacf

Case study of the advanced octagonal cross-section self lifting hybrid tower buckling behavior

Ziteng Wang[a], Rongjun Yang[b], Junqiang Wen[b], Xiangguo Wu[c,d*], Arun Paudel[e], Shuo Zhang[b], Yuncheng Ge[b], Hanyuanbin Wang[f], Kabin Lamichhane[g]

[a] *School of Civil Engineering, Harbin Institute of Technology, Harbin, 150001, China.*
[b] *BCEG Advanced Construction Materials Co., Ltd., Beijing, 100055, China.*
[c] *College of Civil Engineering, Fuzhou University, Fuzhou, 350108, China.*
[d] *Key Lab of Structures Dynamic Behavior and Control of the Ministry of Education, Key Lab of Smart Prevention and Mitigation of Civil Engineering Disasters of the Ministry of the Industry and Information Technology, Harbin Institute of Technology, Harbin, 150090, China. Email:*
[e] *Pulchowk Campus, Institute of Engineering, Tribhuvan University, Kathmandu, Nepal.*
[f] *Wuhan University of Science and Technology, Wuhan, China.*
[g] *Central Material Testing Laboratory, Pulchowk Campus, Institute of Engineering, Tribhuvan University, Kathmandu, Nepal.*

A B S T R A C T

The buckling behavior, as a key issue of the advanced self lifting steel–concrete hybrid tower, was analyzed in this paper. A simplified calculation method and an empirical formula were developed to estimate the critical buckling load of the tower structure. Both linear and nonlinear buckling analyses were performed for hybrid and reinforced concrete towers to identify their buckling modes, failure mechanisms, and weak sections. Case study results indicate that, in the steel–concrete composite system, the steel segment buckles before the concrete portion. For the concrete tower, the midsection (T_3) exhibits earlier buckling than the bottom section, confirming T_3 as the weak buckling zone. The linear buckling critical load was consistently higher than the nonlinear one, with nonlinear analysis providing results closer to realistic conditions. The geometric characteristics of the tower exert a strong influence on its buckling behavior: the critical buckling load increases nonlinearly with the base diameter (D) and wall thickness (t_2), showing diminishing sensitivity at larger values, while it decreases sharply and nonlinearly with the height of the middle concrete section (H_3), indicating a strong adverse effect of slenderness on structural stability. These case study may provide reference for optimizing the geometric design and stability assessment of hybrid wind turbine tower structures.

Keywords: Steel–concrete hybrid tower Buckling stability; Finite element analysis; Nonlinear buckling analysis; Critical buckling load; Parametric analysis

1. Introduction

With the rapid development of wind power technology, the height of wind turbine towers and the length of blades have continued to increase, imposing higher performance demands on tower structures (Ribeiro et al., 2025; Yao et al., 2024). Developing self-lifting super-tall tower structures holds significant engineering importance for solving the technical challenges of lifting at extreme heights (Ruan et al., 2023; Ribeiro et al., 2025). In recent years, the self-lifting structural system has garnered increasing attention in the development of hybrid wind turbine towers (Su et al., 2025). Due to the structural requirements of self-lifting systems, there is a stiffness variation in the vertical direction (Li et al., 2021). Stability has become a crucial criterion in the design and safety assessment of super-high wind power tower cylinders (Shittu et al., 2022). Because wind turbine towers are typically slender, high-rise compression-bending members, instability failure often occurs before material yielding or strength failure (Avci et al., 2025). Especially for self-lifting hybrid towers with vertical stiffness variation, identifying the key factors affecting their overall structural stability is crucial for optimizing

* Corresponding author: Xiangguo Wu (wuxiangguo@hit.edu.cn)

DOI http://dx.doi.org/10.18702/acf.2026.12.3.35

Received: 25-May-2026; Revised: 03-Jul-2026; Accepted: 09-Jul-2026; Published online: 31-Jul-2026

ISSN 2465-7964, eISSN 2465-7972.

design schemes and refining structural details (Ali et al., 2024; Mohammadi et al., 2018). When the external load reaches a certain critical value, the tower may adopt a new equilibrium configuration, indicating the onset of buckling instability (Zhe, 2019). Therefore, an accurate assessment of the buckling stability of wind turbine towers is essential for ensuring structural safety and reliability.

A number of studies have investigated the stability of steel and concrete wind turbine towers through finite element and theoretical analyses. Du Jing et al. (2021) used ANSYS to compare linear and nonlinear buckling of concrete tower and showed that linear buckling overestimates critical loads by neglecting geometric and material nonlinearities. Zhujun (2014) examined the 3 MW steel tower with and without flange connections, demonstrating that inclusion of the P–Δ effect significantly reduces buckling load. Similarly, Yixiong (2012) found that axial compression combined with lateral load increases instability risk. Door openings at the tower base also critically influence buckling behavior. Sahin (2009) and Cheng Haiyan showed that openings weaken tower stiffness, while adding edge stiffeners or reinforcing plates around door openings can improve ultimate strength by about 10%.

Studies have also explored the role of geometric and material characteristics. Rensheng et al. (2011) identified that maximum deflection zones; not necessarily maximum stress zones; represent potential buckling weak points. Jaimes et al. (2020) compared steel and concrete towers, finding that concrete towers offer higher stability and lower cost. Koulatsou et al. (2020) optimized an H120 concrete tower through parametric analysis, determining wall-thickness limits that balance weight and strength. Lee and Bang (2012) analyzed a collapsed tower in Jeju, Korea, estimating the critical buckling load range through nonlinear analysis. Uy and Bradford (1996) developed buckling coefficients for steel–concrete composite plates, offering guidance on calculation lengths. Cao and Li (2012) further showed that local defects at tower top and base reduce stability and that nonlinear analysis yields more realistic critical loads. Collectively, these studies provide valuable insights into tower stability; however, most have concentrated on isolated material systems and idealized geometries. The complex interaction between steel and concrete segments, particularly in hybrid or stepped configurations, remains insufficiently characterized in terms of buckling performance.

Despite these advances, most existing studies have focused on single-material tapered steel towers or homogeneous concrete towers. Research on fabricated steel–concrete hybrid (composite) towers, particularly those with stepped configurations, remains limited. The buckling sensitivity analysis of such composite systems; considering parameters like tower diameter, section height ratio, and wall thickness has not yet been systematically conducted. Moreover, there is a lack of nonlinear buckling simulations, identification of weak buckling zones, and simplified empirical formulas that can be used to estimate the critical buckling load of these self-lifting hybrid towers in practical design.

To address these gaps, this case study investigates the stability performance of a 200-meter (H200) prefabricated steel–concrete composite tower cylinder. The buckling critical load of the stepped hybrid tower is first calculated using theoretical formulations, followed by finite element analyses in ABAQUS for both linear and nonlinear buckling. Based on a comprehensive parametric study, two empirical formulas are developed to predict the buckling critical load more accurately, accounting for real-structure imperfections. The findings provide a scientific basis for stability evaluation and engineering design optimization of high-rise hybrid wind turbine towers. These empirical relations are derived through regression fitting of nonlinear finite element results and subsequently verified against theoretical predictions to ensure their engineering reliability.

2.Materials and Method

This study investigates the overall stability performance of a 200-m-high steel–concrete hybrid wind turbine tower (H200) through a combination of theoretical formulation and numerical simulation. The analysis framework comprises three major steps: (i) formulation of the stability theory and derivation of the critical buckling load for a stepped concrete tower cylinder using the energy method, (ii) implementation of linear and nonlinear buckling analyses in ABAQUS to capture the structural response under increasing load and to identify critical buckling modes, and (iii) comparison between theoretical predictions and finite element results to develop simplified and empirical expressions for estimating the buckling load of tower cylinders. The methodology thus integrates analytical and numerical approaches to reveal the influence of geometric and material parameters on the buckling behavior of the composite tower. To establish the analytical foundation for the numerical simulation, the fundamental theory of stability analysis is first introduced, including the governing equations and assumptions used to determine the critical buckling load of the tower cylinder.

Methods for finite element model processing are not discussed herein and will be addressed in subsequent papers. The present study centers on the global stability performance.

2.1. Stability Analysis Theory

Stability analysis aims to determine the critical load and corresponding buckling mode at which a structure transitions from a stable to an unstable state. The wind turbine tower cylinder behaves as a slender bending member; as external load increases, its stiffness and ability to resist deformation gradually decrease. When the applied load reaches a certain threshold, the overall stiffness of the structure approaches zero, indicating the critical state of instability. A slight lateral disturbance beyond this point can cause sudden buckling failure of the tower. In this study, two stability analysis approaches were employed using ABAQUS—linear buckling analysis and nonlinear buckling analysis.

Linear buckling analysis is an eigenvalue-based method that estimates the theoretical critical load under ideal conditions, assuming perfect geometry and linear elastic behavior. Nonlinear buckling analysis accounts for geometric and material nonlinearities and provides a more realistic prediction of instability by incrementally increasing loads until the structure fails to sustain equilibrium. The nonlinear analysis is therefore used to capture post-buckling response and validate the analytical model (Enchun et al., 2001).

2.1.1. Linear Buckling Analysis Theory

Linear buckling analysis, also referred to as eigenvalue buckling analysis, is based on small-displacement linear theory and determines the load factor at which the stiffness matrix of the structure becomes singular. Assuming that the external load mode of the structure is$P$, the amplitude isλ), and the internal force of the structure isQ, the static balance equation will be:

$$\lambda P = \lambda Q \tag{1}$$

Similarly, the equilibrium equation of the structure under $(\lambda + \Delta\lambda)P$ load will be:

$$\left\{\left[K^E\right]+\left[K^S\left(S+\lambda\Delta S\right)\right]+\left[K^G\left(u\right)+\lambda\Delta u\right]\right\}\Delta u = \Delta\lambda P \tag{2}$$

Likewise, when the structure reaches the critical load to maintain stability that is,$\Delta\lambda$=0, substituting this, equation (2) will be,

$$\left\{[K]+\lambda[S]\right\}\Delta u = 0 \tag{3}$$

Where$[K]$——Stiffness matrix ;
$[S]$——Stress stiffness matrix ;
Δu——Displacement eigenvector ;
λ——Critical load factor for buckling instability。

2.1.2. Nonlinear Buckling Analysis Theory

Nonlinear buckling analysis incorporates geometric and material nonlinearity and considers the entire load history during deformation. Unlike linear analysis, the stiffness matrix continuously updates to reflect changes in geometry as the load increases. The general nonlinear buckling eigenvalue equation can be expressed as:

$$\left[K+\lambda\Delta K^G\left(\Delta u,u,\Delta\sigma\right)\right]-\Delta u = 0 \tag{4}$$

Where ΔK^G——Geometric stiffness matrix ;
K——Tangential stiffness matrix.
Buckling instability load is :

$$P_{cr} = P_{i-1}+\lambda\Delta P_{i-1} \tag{5}$$

Where P_{i-1}——Load from increment step ;
ΔP_{i-1}——Load increment in increment step ;
P_{cr}——The structural instability load calculated from the buckling load increment extracted after the end of the i-step incremental analysis.

2.2. Analytical Determination of Critical Load of a Stepped Concrete Tower

Before performing the finite element stability analysis, an analytical approach was first developed to estimate the theoretical critical buckling load of the stepped concrete tower cylinder. The objective of this step was to establish a baseline understanding of the tower's buckling behavior under idealized conditions, which would later be compared with numerical simulation results for validation and refinement. The critical load of a compression member with multi-step variable cross-sections (Figure 1) was determined using the energy method, following the formulations proposed by Weiping (1998) and Huiqiang and Laide (1995). The calculation procedure is outlined below.

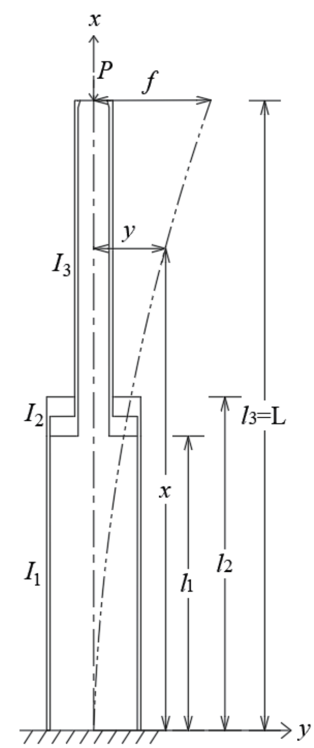

Figure 1 Calculation diagram of concrete tower cylinder

Assuming that the cantilever compression rod with one end fixed and one end free is unstable, the winding curve is:

$$y = f\left(1-\cos\left(\frac{\pi x}{2L}\right)\right) \tag{6}$$

After differentiating the equation, equation (6) will be:

$$y' = \frac{f\pi}{2L}\sin\left(\frac{\pi x}{2L}\right) \tag{7}$$

The external work W of the axial force P on the vertical displacement of the compression bar is:

$$\begin{aligned} W &= P\cdot\zeta = P\cdot\frac{1}{2}\cdot\int_0^L \left(y'\right)^2 dx \\ &= \frac{P}{2}\int_0^L\left(\frac{f\pi}{2L}\sin\left(\frac{\pi x}{2L}\right)\right)^2\cdot\frac{2L}{\pi}d\frac{\pi x}{2L} = P\cdot\frac{f^2\pi^2}{16L} \end{aligned} \tag{8}$$

The number of variable section sections of the concrete tower section of this structure is 3, and the deformation energy of section i is U_i。

$$
\begin{aligned}
U_i &= \frac{1}{2}\int_{l_{i-1}}^{l_i} EI_i (y'')^2 dx = \frac{EI_i}{2}\int_{l_{i-1}}^{l_i}\left(\frac{f\pi^2}{4L^2}\right)^2 \cos^2\left(\frac{\pi x}{2L}\right)dx \\
&= \frac{f^2\pi^4 EI_i}{64L^3}\left[\frac{l_i}{L}-\frac{l_{i-1}}{L}+\frac{1}{\pi}\left(\sin\left(\frac{l_i}{L}\pi\right)-\sin\left(\frac{l_{i-1}}{L}\pi\right)\right)\right]
\end{aligned}
\tag{9}
$$

Then the total bending strain energy U of the structure with three sections of variable cross-section compression bar is:

$$
\begin{aligned}
U &= \sum_{i=1}^{3} U_i \\
&= \frac{f^2\pi^4 EI_i}{64L^3}\sum_{i=1}^{3}\frac{I_i}{I_1}\left[\frac{l_i}{L}-\frac{l_{i-1}}{L}+\frac{1}{\pi}\left(\sin\left(\frac{l_i}{L}\pi\right)-\sin\left(\frac{l_{i-1}}{L}\pi\right)\right)\right]
\end{aligned}
\tag{10}
$$

According to the principle of energy conservation, the external force work W when the compression bar is bent should be equal to the bending strain energy U, that is, $W=U=U_1+U_2+U_3$. The critical force F_{cr} obtained from the simultaneous equation is :

$$
F_{cr} = \frac{\pi^2 EI_1}{4\mu L^2} \tag{11}
$$

Where : μ——Converted length coefficient of compression bar with multi-step deformation section, and the calculation formula is :

$$
\mu = \frac{1}{\sum_{i=1}^{3}\frac{I_i}{I_1}\left[\frac{l_i}{L}-\frac{l_{i-1}}{L}+\frac{1}{\pi}\left(\sin\left(\frac{l_i}{L}\pi\right)-\sin\left(\frac{l_{i-1}}{L}\pi\right)\right)\right]} \tag{12}
$$

The parameters required for calculation are shown in Table 1.

Table 1 Calculation parameters of typical tower cylinder

Parameter symbol	Dimensions (mm)	Parameter symbol	Dimensions (mm4)
l_1	84000	I_1	3.222E+14
l_2	90000	I_2	1.776E+15
L	166000	I_3	1.984E+13

According to formula (12)μ=1.1644, and according to formula (11), $F_{cr}=8.0873\times10^8$N, According to the following text, the finite element calculation result is 2.7748×10^8N. It can be observed that the theoretically predicted critical buckling load is notably higher than that obtained from finite element (FE) analysis. The primary discrepancy arises from the inherent limitation of the adopted analytical formula (Eq. (6)): this expression assumes the maximum curvature occurs at the fixed end (x=0) while the curvature vanishes at the free end (x=L) with zero bending moment. However, the concrete tower is a tapered member with a smaller cross-sectional moment of inertia at the top relative to lower segments. Under physical elastic buckling, the extremely low flexural stiffness at the tower top induces substantially larger curvature deformation at this position compared with the base. The analytical solution fails to fully capture this phenomenon and consequently underestimates the bending strain energy at the top, leading to an overprediction of the critical buckling load.

Furthermore, the tower structure is highly sensitive to geometric imperfections such as door openings, which further degrade its actual critical load capacity. Since the theoretical algorithm excludes such structural defects, its predicted critical load is unconservative. For this reason, the analytical solution is only used herein for qualitative comparison rather than as a quantitative basis for conclusions. All subsequent quantitative analyses, parametric investigations, and design recommendations regarding critical buckling loads rely exclusively on FE results that incorporate geometric nonlinearity, initial geometric imperfections, and contact nonlinearity. Such FE predictions better reflect practical engineering conditions and yield conservative, reliable outcomes.

3. Results and Discussions

3.1. Linear Buckling Analysis Results

In the linear buckling analysis, an axial load of 10^6 N was applied at the top reference point of the tower cylinder, and the effect of the door opening was included in the model. For linear buckling analysis, nonlinear factors are not considered. Due to the complex stress of the tower cylinder itself, there are a variety of load combinations, and the most significant influence on the buckling of the tower cylinder is the axial force and transverse bending moment. Therefore, the analysis adopted a purely vertical axial load condition, and the critical buckling load was obtained by multiplying the first-order buckling eigenvalue by the applied reference load of 10^6 N. In the ABAQUS finite element model, the linear buckling analysis was performed using a linear perturbation step, which extracts the buckling eigenvalues and corresponding mode shapes. The first-order buckling modes of the steel–concrete composite tower cylinder and the plain concrete tower cylinder without a steel tube are shown in Figure 2.

The first-order eigenvalue for the steel–concrete composite tower cylinder was 140.78, corresponding to a critical buckling load of 1.4078×108 N. For the concrete tower cylinder without the steel tube, the first-order eigenvalue was 277.48, giving a critical buckling load of 2.7748×108 N. These results indicate that the steel–concrete composite tower exhibits a lower buckling resistance compared with the concrete-only tower, implying that under axial compression, the steel section is more prone to buckle before the concrete portion.

The first-order eigenvalue for the steel–concrete composite tower cylinder was 140.78, corresponding to a critical buckling load of 1.4078×108 N. For the concrete tower cylinder without the steel tube, the first-order eigenvalue was 277.48, giving a critical buckling load of 2.7748×108 N. These results indicate that the steel–concrete composite tower exhibits a lower

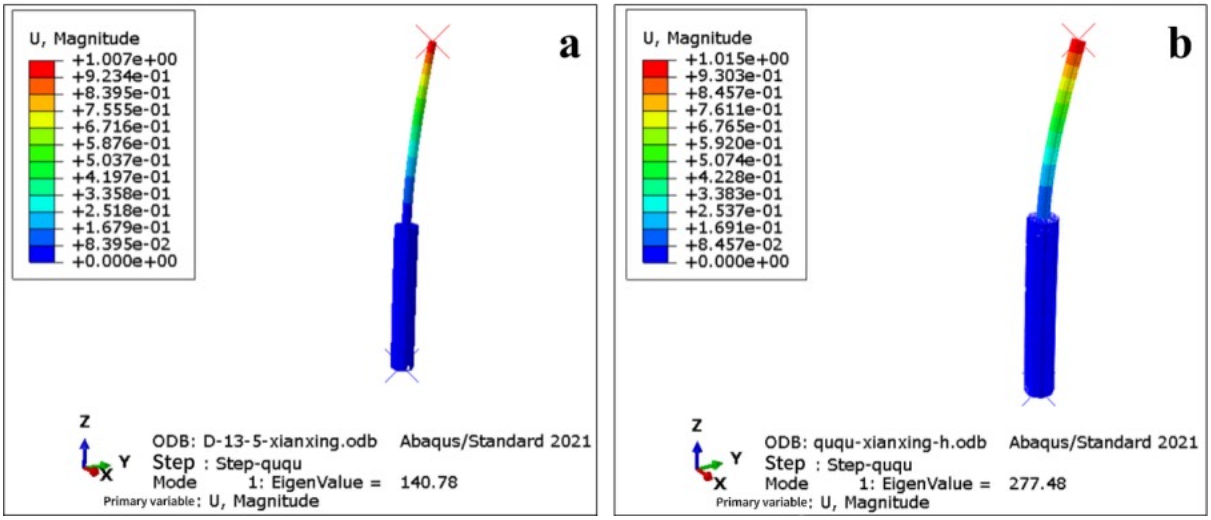

Figure 2 First order mode shape diagram of tower cylinder linear buckling analysis: (a) Linear buckling of steel concrete composite tower cylinder and (b) Linear buckling of concrete tower structure

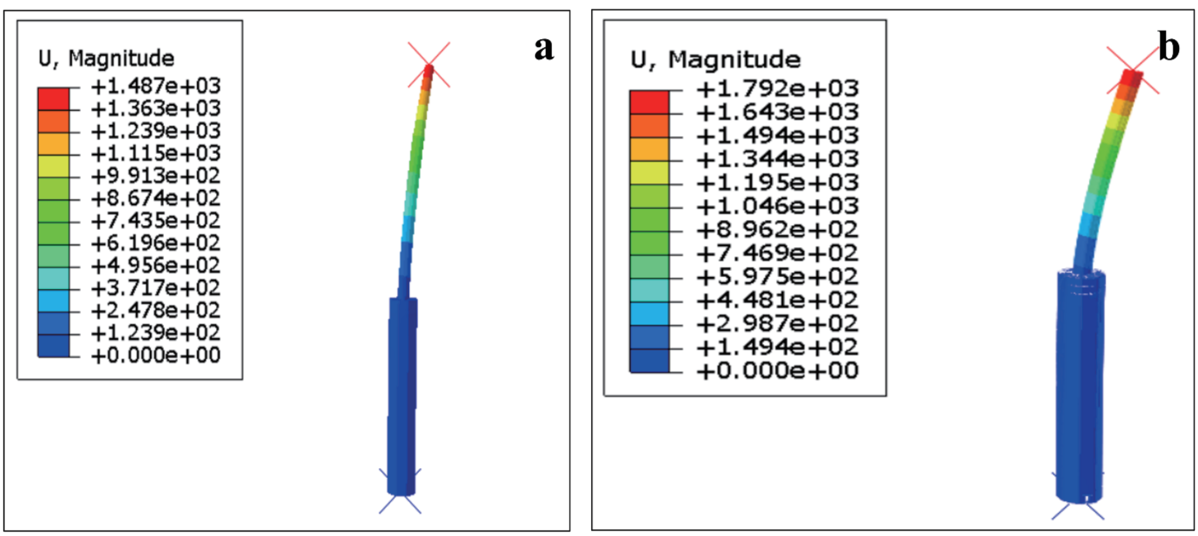

Figure 3 First order mode shape diagram of tower cylinder linear buckling analysis: (a) Linear buckling of steel concrete composite tower cylinder and (b) Linear buckling of concrete tower structure

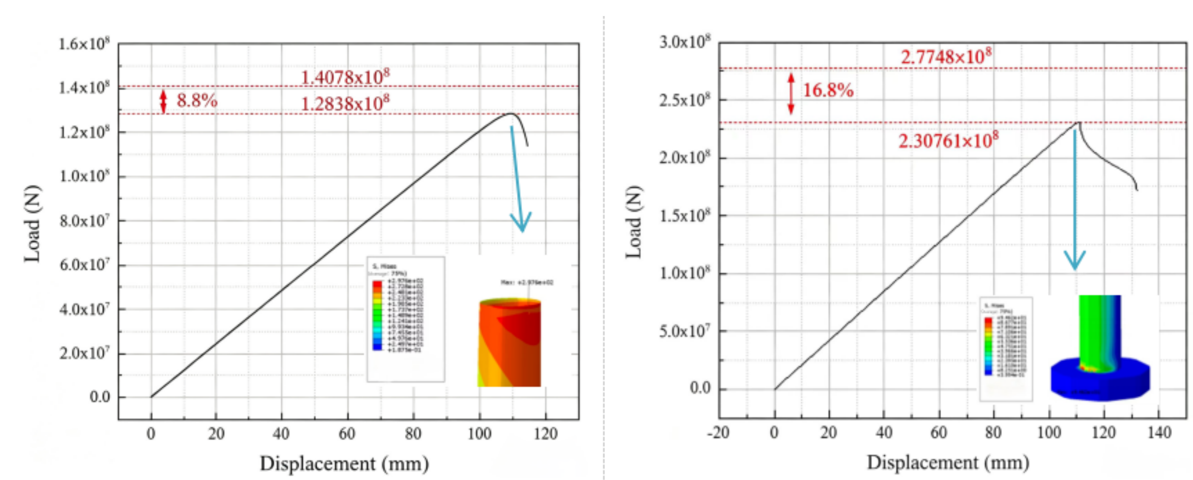

Figure 4 Tower cylinder load-displacement curve: (a) Nonlinear buckling of steel concrete composite tower cylinder and (b) Nonlinear buckling of concrete tower cylinder structure

buckling resistance compared with the concrete-only tower, implying that under axial compression, the steel section is more prone to buckle before the concrete portion.

3.2. Nonlinear Buckling Analysis Results

Compared with linear buckling analysis, nonlinear buckling analysis is more accurate because it considers both material and geometric nonlinearity, and the calculated nonlinear buckling critical load is generally less than the linear buckling critical load. The nonlinear buckling analysis in ABAQUS is based on the linear buckling analysis by adding the concrete material constitutive model, that is, considering the material nonlinearity and opening the geometric large deformation to consider the geometric nonlinearity. The Static-Risk analysis step is used in the analysis step, and the applied load can be slightly larger than the critical load obtained from the linear buckling. The analysis results are shown in Figure 3. According to the vibration mode diagram, significant buckling deformation occurs in the upper regions of both the concrete and steel tower sections. The nonlinear buckling analysis further provides the corresponding load–displacement response of the tower cylinder. As shown in Figure 4, according to the curve, the nonlinear buckling critical load of the steel-concrete composite tower is 1.28×10^{8} N, about 8.8% less than the linear buckling critical load. The position where the maximum stress and buckling deformation occur is the top of the steel cylinder, that is, the steel cylinder will buckle before the concrete cylinder. The parametric analysis in this paper only focuses on the concrete tower segment. Accordingly, only the 166 m concrete tower section is selected as the research object, and the steel tower segment is excluded from the parametric investigation.The nonlinear buckling critical load of concrete tower cylinder is 2.3×10^{8} N, which is about 16.8% less than the linear buckling critical load. The maximum stress and buckling deformation occur in the lower region of the T3 section. This indicates that the mid-height concrete portion of T3 will buckle earlier than the bottom section, confirming T3 as a relatively thin and weak segment prone to instability. According to the analysis results, it can be seen that the nonlinear buckling critical load of the tower is less than the linear buckling critical load, indicating that the material and geometric nonlinearity of the structure have a great impact on the buckling critical load of the structure. Therefore, it is necessary to carry out nonlinear buckling analysis in the design of the thin-walled slender structure of wind tower.

3.3. Factors Affecting Tower Stability

3.3.1. Diameter of Bottom Concrete Section

This section aims to explore the impact of the bottom concrete tower cylinder diameter D on the overall stability of the concrete tower cylinder. The concrete tower cylinder diagram is depicted in Figure 5. Six types of tower models with tower cylinder diameter D=12m, 12.5m, 13m, 13.5m, 14m and 14.5m are established. The model parameter table is shown in Table 2. The influence of the bottom diameter on the critical buckling load of the concrete tower cylinder is explored. The linear buckling analysis of six types of tower is carried out (Figure 6).

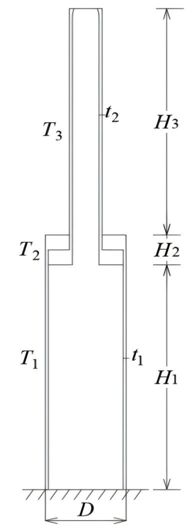

Figure 5 Schematic diagram of concrete tower cylinder

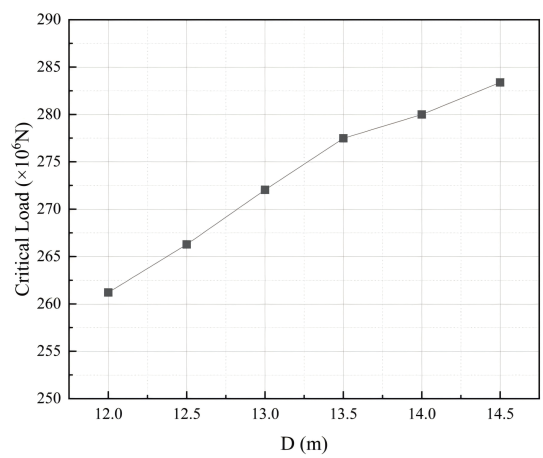

Figure 6. Variation of buckling critical load ($\times10^{6}$) with diameter D

Taking the 12 m diameter and corresponding buckling load of 261.20 $\times$ 10^{6} N as the reference, the analysis shows that the critical buckling load increases gradually with the rise in diameter, but at a decreasing rate. When the diameter is increased by 4.17 %, the buckling load increases by only 1.95 %, and at a 20.83 % increase in diameter (from 12 m to 14.5 m), the buckling load rises by about 8.49 %. This indicates that the relationship between diameter and buckling resistance is nonlinear and exhibits diminishing sensitivity; that is, larger increments in diameter yield progressively smaller proportional gains in buckling capacity. On average, the sensitivity ratio (percentage increase in load per percentage increase in diameter) is approximately 0.4, meaning that a 1 % increase in diameter results in about a 0.4 % increase in critical buckling load. Mechanically, increasing the diameter enhances the radius of gyration and second moment of area, thereby improving global flexural stiffness

Table 2 Parameters of six kinds of diameter tower cylinder

Tower cylinder model	D（m）	H_1（m）	H_2（m）	H_3（m）	t_1（mm）	t_2（mm）
D12.0-$H_1$84-$H_3$76	12.0	84	6	76	300	300
D12.5-$H_1$84-$H_3$76	12.5	84	6	76	300	300
D13.0-$H_1$84-$H_3$76	13.0	84	6	76	300	300
D13.5-$H_1$84-$H_3$76	13.5	84	6	76	300	300
D14.0-$H_1$84-$H_3$76	14.0	84	6	76	300	300
D14.5-$H_1$84-$H_3$76	14.5	84	6	76	300	300

Table 3 Parameters of tower drum with five H3 heights

Tower cylinder model	D（m）	H_1（m）	H_2（m）	H_3（m）	t_1（mm）	t_2（mm）
D13.5-$H_1$92-$H_3$68	13.5	92	6	68	300	300
D13.5-$H_1$88-$H_3$72	13.5	88	6	72	300	300
D13.5-$H_1$84-$H_3$76	13.5	84	6	76	300	300
D13.5-$H_1$80-$H_3$80	13.5	80	6	80	300	300
D13.5-$H_1$76-$H_3$84	13.5	76	6	84	300	300

and classical buckling strength (Ma et al., 2020). However, as the tower cylinder becomes larger in diameter, the diameter-to-thickness ratio (D/t) also rises, amplifying imperfection sensitivity and the likelihood of local shell buckling (Lee et al., 2001; Takano et al., 2021). Consequently, the beneficial effect of diameter enlargement is offset by the structure’s increasing susceptibility to geometric imperfections and mode interaction, causing the observed gain in buckling load to be modest and nonlinear. This trend suggests that while increasing the base diameter contributes to improved stability, its efficiency diminishes beyond a certain size, as stiffness gains plateau relative to geometric expansion.

3.3.2. Height of Top Steel Section

Since the T_3 tower cylinder is identified as a weak section prone to buckling, the influence of varying its height (H_3) on the overall stability of the concrete tower is investigated. By adjusting the H_3 height, the analysis evaluates how changes in this geometric parameter affect the tower’s critical buckling load and deformation behavior, thereby clarifying the sensitivity of the structure’s stability to height variation. Five types of tower cylinder models with T_3 tower cylinder height H_3=68m, 72m, 76m, 80m and 84m are established, and the model parameters are shown in Table 3.

Taking the T_3 tower cylinder height of 68 m and its corresponding buckling load of 316.91 × 10^6 N as the reference, the analysis reveals that the critical buckling load decreases progressively with increasing height. When the height increases by 5.9 % (to 72 m), the buckling load drops by about 8.6 %, and at a 23.5 % increase in height (to 84 m), the load decreases by nearly 29 % (Figure 7). This clearly indicates a strong inverse relationship between height and buckling resistance, where taller configurations lead to significantly reduced stability. The relationship is nonlinear, with the reduction rate becoming stronger as height increases, reflecting the amplifying effects of global slenderness and flexural deformation.

Increasing the height of the tower increases its slenderness ratio (L/r), which intensifies the susceptibility to global buckling and mode interaction between flexural and local shell instability (Goel, 2021). A taller structure not only experiences larger bending moments due to lateral wind loads but also exhibits greater geometric imperfection sensitivity, leading to a sharper reduction in effective stiffness and load-carrying capacity (Chen et al., 2021). Similar findings have been reported in parametric stability analyses of wind turbine towers, where increased height or unsupported length was shown to markedly lower the global buckling capacity (Ma et al., 2020; Koulatsou et al., 2019). This study thus reinforces that height is the most dominant and adverse geometric parameter for the stability of the T_3 tower cylinder, as excessive vertical extension amplifies slenderness-induced instability and accelerates buckling onset even under modest increases in overall height.

Table 4 parameters of tower drum with five t2 thicknesses

Tower cylinder model	D（m）	H_1（m）	H_2（m）	H_3（m）	t_1（mm）	t_2（mm）
t_2-220	13.5	84	6	76	300	220
t_2-240	13.5	84	6	76	300	240
t_2-260	13.5	84	6	76	300	260
t_2-280	13.5	84	6	76	300	280
t_2-300	13.5	84	6	76	300	300

3.3.3. Wall Thickness of Top Steel Section

This analysis investigates the influence of varying the steel section thickness (t_2) on the stability of the concrete tower. Five types of tower drum models with T_3 tower drum thickness t_2=220mm, 240mm, 260mm, 280mm and 300mm are established. The basic model of tower drum is D13.5-H184-$H_3$76, and only t_2 of the model is changed. The model parameters are shown in Table 4.

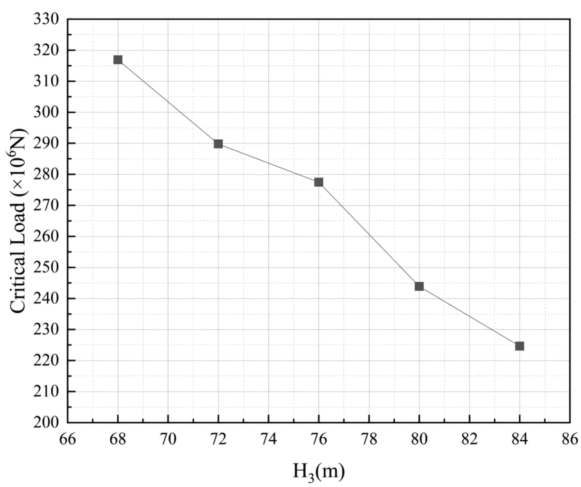

Figure 7 Variation of buckling critical load with H_3

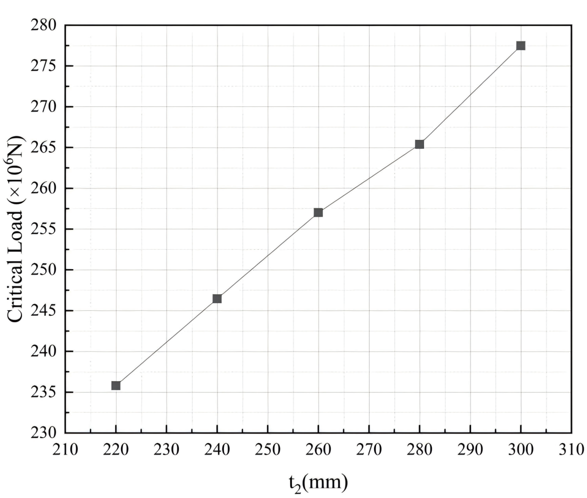

Figure 8 Variation of buckling critical load with t_2

Starting from a wall thickness of 220 mm with a corresponding critical buckling load of 235.80 × 10^6 N, the results show a clear enhancement in structural stability as the section becomes thicker. Increasing the thickness to 300 mm, which represents a 36 % rise, results in an approximate 17.7 % improvement in the buckling load, reaching 277.48 × 10^6 N (Figure 8). Unlike the influence of height, where the effect was strongly negative, the increase in thickness contributes positively but with a gradually diminishing rate of gain. The improvement in buckling resistance between successive increments becomes smaller as the section thickens, indicating a nonlinear strengthening behavior.

Increasing the wall thickness reduces the diameter-to-thickness ratio (D/t), which in turn enhances local shell buckling resistance and increases both axial and bending stiffness of the tower (Takano et al., 2021). This behavior aligns with classical shell theory, where a lower D/t ratio suppresses local buckling waves and delays the onset of instability (Maharditiya et al., 2025). However, as the section becomes thicker, the structure gradually transitions from a shell-dominated response toward a plate-like behavior with reduced sensitivity to additional thickening (Lee et al., 2001). Consequently, the incremental stability gains taper off beyond a certain limit, producing a nonlinear but saturating trend. This observation underscores that while increasing thickness is beneficial for improving the buckling capacity of the T_3 tower segment, excessive thickening may lead to material inefficiency with only marginal structural benefit.

3.4. Empirical Formula for Buckling Critical Load

3.4.1. Case-I

To develop an empirical relationship suitable for preliminary design, a series of parametric models were analyzed by varying the slenderness ratio (μ). The corresponding critical buckling loads obtained from the finite element analysis and theoretical calculation based. on Equation (11) are depicted in Figure 9. Finite element results demonstrate a clear decreasing trend of critical load with increasing μ, indicating that the overall buckling capacity of the tower cylinder diminishes as the structure becomes slenderer. This trend is consistent with the mechanical expectation that higher slenderness ratios lead to reduced stiffness and greater susceptibility to instability under axial compression.

The variation trend is illustrated in Figure 9, where the theoretical curve overestimates the critical load compared to the finite element results. This discrepancy arises because the theoretical formulation neglects imperfections, residual stresses, and local geometric deviations present in the actual structure. To improve its applicability, a correction coefficient c1 was introduced into the theoretical equation (Eq. 11), yielding a modified standard form expressed as Equation (13):

$$F_{cr} = c_1 \cdot \frac{\pi^2 EI_1}{4\mu L^2} \tag{13}$$

Linear regression (y=c1x) was performed between the finite element (y) and theoretical results (x). The analysis produced a best-fit coefficient of c1=0.32521, as shown in Figure 10, which significantly enhances the agreement between the predicted and simulated buckling capacities. Consequently, the refined empirical relationship (Eq. 14) provides a practical means for estimating the buckling critical load of stepped concrete–steel composite tower cylinders with acceptable engineering accuracy.

$$F_{cr} = 0.32521 \cdot \frac{\pi^2 EI_1}{4\mu L^2} = 0.0813 \frac{\pi^2 EI_1}{\mu L^2} \tag{14}$$

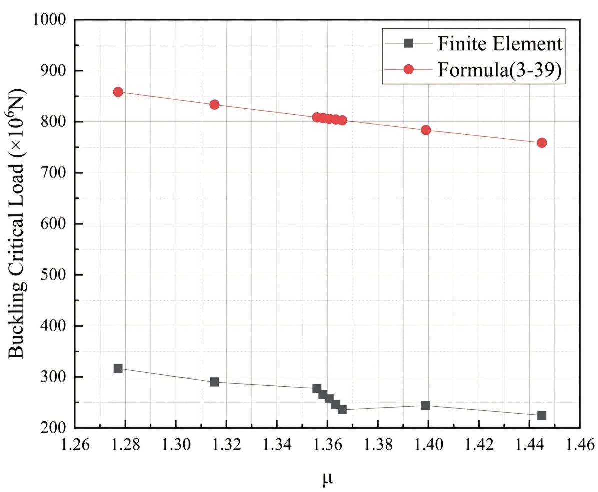

Figure 9 Variation of buckling critical load with μ value

It can be observed that the fitting coefficient remains relatively low. The fundamental reason is that all theoretical formulas are derived based on the Euler cantilever beam, whose buckling mode assumes zero curvature at the free end. However, the tapered tower studied in this paper possesses a much smaller moment of inertia at the top than at the base. During actual buckling, the curvature at the tower top is far larger than that at the bottom, which leads to an essential difference between the two deformation modes.

Consequently, the theoretical value serves as a rigid upper bound that is considerably higher than the real load capacity, and a reduction of approximately 0.3 orders of magnitude is required to approach the true value. The proposed formula is only applicable to the specific structural type and parameter range investigated herein. The resulting empirical formula is merely adopted for rapid estimation during the conceptual design stage. All quantitative conclusions are based on finite element analysis results that account for geometric nonlinearity, initial imperfections and contact nonlinearity. The finite element predictions are conservative and reliable for engineering applications.

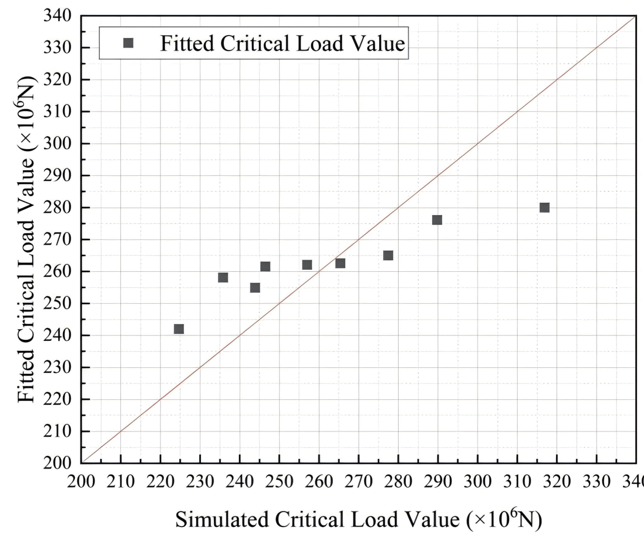

Figure 10 Fitting result curve

3.4.2. Case-II

In the second approach, the critical buckling load is determined using the classical Euler formulation, as expressed in Equation (15). For a cantilever-type tower cylinder, the effective boundary condition factor is taken as μ0=2. To adapt the Euler expression to the present composite section, the section moment of inertia (i) is replaced by an equivalent moment of inertia that accounts for the material heterogeneity and sectional interaction between steel and concrete, as shown in Equation (16). Using this modification, the theoretical critical load is obtained as 8.0347×10^8 N, which is in close agreement with the value derived from the energy method in Equation (11).

$$F_{cr} = \frac{\pi^2 EI}{(\mu_0 L)^2} = \frac{\pi^2 EI}{4L^2} \tag{15}$$

$$I = I_1 \times \frac{H_1}{L} + I_2 \times \frac{H_2}{L} + I_3 \times \frac{H_3}{L} \tag{16}$$

The trend shown in Figure 11 indicates that the critical buckling load increases with the equivalent linear stiffness (i), as expected, but the theoretical predictions remain consistently higher than the finite element results. This discrepancy arises because the theoretical Euler formulation neglects the effects of geometric imperfections, residual stresses, and boundary discontinuities inherent in the actual tower cylinder. To enhance the applicability of the analytical model, a correction coefficient c2 was introduced in a linear regression relation (y=c2x) to modify Equation (15). The adjusted relationship was expressed in standard linear form as Equation (17):

$$F_{cr} = c_2 \cdot \frac{\pi^2 EI}{4L^2} \tag{17}$$

A linear regression was then performed between the theoretical and finite element data (Figure 11), yielding a best-fit correction coefficient of c2=0.32699. The fitted correlation is shown in Figure 12, demonstrating strong agreement between the empirical and simulated results. Accordingly, the refined empirical equation, presented as Equation (18), provides an efficient and reliable tool for preliminary estimation of the buckling critical load of stepped composite tower cylinders:

$$F_{cr} = 0.32699 \cdot \frac{\pi^2 EI}{4L^2} = 0.0817\frac{\pi^2 EI}{L^2} \tag{18}$$

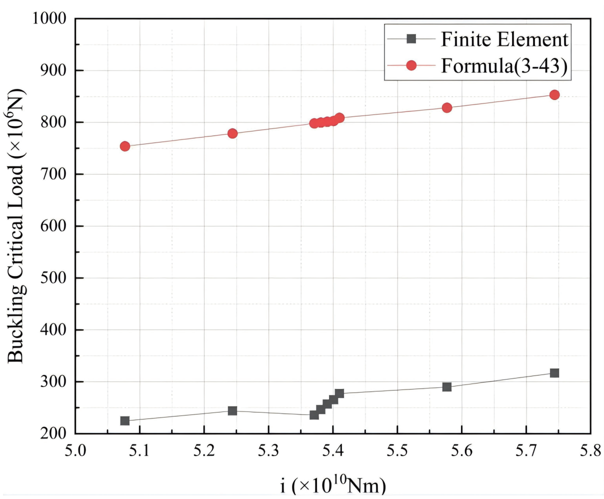

Figure 11 Variation of buckling critical load with i value

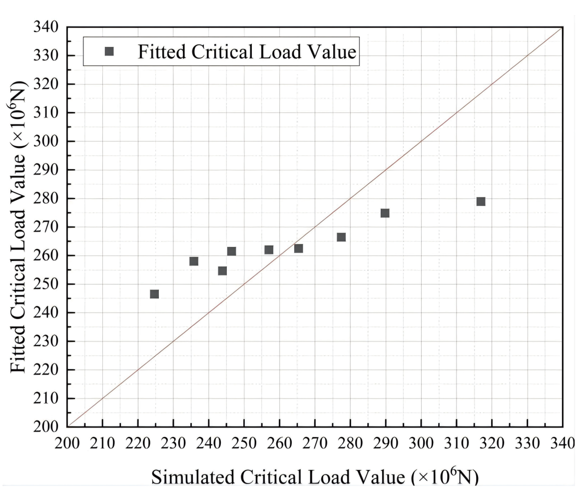

Figure 12 Fitting result curve

4. Conclusion

This study addressed the limited understanding of the buckling stability of prefabricated steel–concrete hybrid wind turbine towers, particularly those with stepped configurations, for which systematic analyses and design-oriented prediction models have been lacking. Focusing on a 200-meter (H200) hybrid tower cylinder, the research combined analytical and numerical approaches to bridge this gap. A simplified theoretical algorithm and two empirical formulations for estimating the critical buckling load were developed and calibrated through ABAQUS-based finite element simulations that account for geometric nonlinearity and sectional interaction effects. By comparing theoretical, numerical, and regression-based results, the study quantified the deviation between idealized analytical predictions and real-structure performance, thereby providing an improved and practically applicable framework for the stability evaluation and design optimization of hybrid wind turbine towers. The principal findings are summarized as follows:

1. General key controlling segment for anti-buckling solution: The buckling behavior analysis revealed that instability in the steel–concrete composite tower initiates in the upper steel segment before the concrete portion, primarily because the steel shell has a higher slenderness ratio and lower local stiffness under compressive bending. In contrast, for the pure concrete tower, the middle section (T_3) exhibited the earliest deformation due to accumulated axial compression combined with flexural bending from self-weight and wind moment redistribution, making it the weakest and most buckling-prone region. The nonlinear buckling load was consistently lower than the linear estimate, confirming that material nonlinearity, geometric imperfection, and boundary conditions substantially reduce the actual load-bearing capacity compared to idealized predictions.

2. Key geometric parameters for the prefabricated tower segmental interegal analysis and optimization: The geometric configuration of the tower cylinder strongly governs its stability characteristics. The critical buckling load increases nonlinearly with the tower base diameter and the wall thickness of the middle concrete section (t2), exhibiting diminishing sensitivity as stiffness gains plateau. In contrast, increasing the height of the middle section (H3) produces a nonlinear but progressively sharper reduction in buckling capacity, reflecting the amplifying influence of slenderness and global deformation effects.

3. Empirical model development: The finite element results were consistently lower than the theoretical predictions due to the idealizations inherent in analytical methods, which neglect fabrication imperfections, openings, and residual stresses. To address this limitation, two empirical correction formulas were established based on regression analysis, enabling more reliable preliminary estimation of the buckling critical load for stepped steel–concrete tower cylinders.

Acknowledgments

The research described in this paper was financially supported by the National Natural Science Foundation of China (Grant No. 52178195) and the Project Key Technology Research on Ultra High Performance Concrete (UHPC) Wind Power

Hybrid Tower System (Project No. SA10000003512023054).

Declaration of Interest Statement

The authors declare that they have no known competing financial interests or personal relationships that could have influenced the work reported in this study.

References

[1] Ali, S., Park, H., & Lee, D. (2024). Structural optimization of vertical axis wind turbine (VAWT): A multivariable study for enhanced deflection and fatigue performance. Journal of Marine Science and Engineering, 13(1), 19.

[2] Avc1, B., Bilgin, E., & Tüfekci, E. (2025, May). Structural and dynamic analysis of wind turbine towers: A simplified 1D modeling approach. In Proceedings of the ASME Aerospace Structures, Structural Dynamics, and Materials Conference (Vol. 88759, p. V001T01A013). American Society of Mechanical Engineers.

[3] Cai, Z. (2014). Seismic response and nonlinear stability analysis of wind turbine tower cylinder [Master’s thesis, Xi’an University of Technology].

[4] Cao, Q., Li, Y., & Zhang, H. (2012). Nonlinear buckling analysis of wind turbine towers. Advanced Materials Research, 383, 6469–6475.

[5] Cheng, H. (2009). Finite element analysis of MW wind turbine tower [Master’s thesis, Chongqing University].

[6] Du, J., Yang, R., Li, D., & Xu, Y. (2021). Stability analysis of reinforced concrete tower cylinder of MW wind turbine. Journal of Solar Energy, 42(3), 9–14.

[7] He, Z. (2019). Multi-objective optimization research on structural parameters of megawatt wind turbine tower [Master’s thesis, Lanzhou University of Technology].

[8] Jaimes, M. A., García-Soto, A. D., del Campo, J. O. M., & Hernández-Barrientos, J. (2020). Probabilistic risk assessment of wind turbine towers subjected to cyclone-induced wind loads. Wind Energy, 23(3), 528–546.

[9] Koulatsou, K. G., Chondrogiannis, K. A., & Gantes, C. J. (2019, October). Structural optimization of tubular steel wind turbine towers with respect to buckling. In Proceedings of the IASS Annual Symposium 2019 (No. 17, pp. 1–8). International Association for Shell and Spatial Structures.

[10] Koulatsou, K. G., Chondrogiannis, K. A., & Gantes, C. J. (2020). Resonance investigation and its effects on weight optimization of tubular steel wind turbine towers. Procedia Manufacturing, 44, 4–11.

[11] Lee, K. S., & Bang, H. J. (2012). Prediction of lateral buckling load for wind turbine tower structures. International Journal of Precision Engineering and Manufacturing, 13(10), 1829–1836.

[12] Li, Z., Chen, H., Xu, B., & Ge, H. (2021). Hybrid wind turbine tower optimization using a parallel updated particle swarm algorithm. Applied Sciences, 11(18), 8683.

[13] Liu, Y. (2012). Dynamics and stability analysis of large wind turbine tower tube [Master’s thesis, Lanzhou University of Technology].

[14] Ma, Y., Martinez-Vazquez, P., & Baniotopoulos, C. (2020). Buckling analysis for wind turbine tower design: Thrust load versus compression load based on energy method. Energies, 13(20), 5302.

[15] Maharditya, A. R., Ganendra, B., Yaningsih, I., Prabowo, A. R., Ehlers, S., Braun, M., & Wijaya, R. (2025). Buckling behavior of thin-walled cylindrical shell structures under axial compression: Effects of imperfection parameters using finite element analysis. Journal of Umm Al-Qura University for Engineering and Architecture, 1–24.

[16] Mohammadi, M. R. S., Richter, C., Pak, D., Rebelo, C., & Feldmann, M. (2018). Steel hybrid onshore wind towers installed with minimal effort: Development of a lifting process. Wind Engineering, 42(4), 335–352.

[17] Ribeiro, J. A., Ribeiro, B. A., Pimenta, F., Tavares, S. M., Zhang, J., & Ahmed, F. (2025). Offshore wind turbine tower design and optimization: A review and AI-driven future directions. Applied Energy, 397, 126294.

[18] Ruan, R., Lai, M., Jiang, C., Wang, J., & Lin, Y. (2023). Integral lifting of steel structure corridors between two super high-rise buildings under wind load. Buildings, 13(10), 2441.

[19] Sahin, S. (2009). Wind turbine tower structural analysis under wind loading with respect to cost [Master’s thesis, University of Liège].

[20] Shittu, A. A., Mehmanparast, A., Amirafshari, P., Hart, P., & Kolios, A. (2022). Sensitivity analysis of design parameters for reliability assessment of offshore wind turbine jacket support structures. International Journal of Naval Architecture and Ocean Engineering, 14, 100441.

[21] Su, B., Guo, T., & Alam, M. M. (2025). A review of wind energy harvesting technology: Civil engineering resources, theory, optimization, and applications. Applied Energy, 389, 125771.

[22] Uy, B., & Bradford, M. A. (1996). Elastic local buckling of steel plates in composite steel–concrete members. Engineering Structures, 18(3), 193–200.

[23] Wu, W. (1998). Calculation of critical force of cantilever compression bars with stepped deformation sections. Journal of Jiangxi Institute of Education (Natural Science), (6), 29–30.

[24] Yao, Y., Yu, C., Rao, M., Wang, Z., Hua, X., & Chen, C. (2024). Dynamic characteristics of a wind turbine tower based on wind tunnel experiments. Energies, 17(16), 4080.

[25] Zheng, H., & Shi, L. (1995). Calculation of critical load of cantilever compression bars with stepped deformation sections. Mechanical Design, (1), 18–29.

[26] Zhu, E., Mandal, P., & Calladine, C. R. (2001). Buckling analysis of thin cylindrical shells under axial compression. Journal of Civil Engineering, (3), 18–22.

[27] Zhu, R., Liu, Y., Jiang, D., Chen, J., An, X., Liu, C., & Chen, C. (2011). Finite element analysis of MW wind turbine towers. Mechanical Design and Manufacturing, (5), 104–106.